Acta Biochim Biophys Sin, 2016, 48(4), 342–353
doi: 10.1093/abbs/gmw011
Advance Access Publication Date: 8 March 2016
Original Article

Original Article

Resveratrol protects PC12 cells against OGD/R-induced apoptosis via the mitochondrial-mediated signaling pathway

Xuan Liu[1,†], Xiangyang Zhu[2,†], Miao Chen[1], Qinmin Ge[1], Yong Shen[1], and Shuming Pan[1,*]

[1]Department of Emergency, Xinhua Hospital, Shanghai Jiao Tong University School of Medicine, Shanghai 200092, China, and [2]Division of Nephrology and Hypertension, Mayo Clinic, Rochester, MN 55905, USA

[†]These authors contributed equally to this work.

*Correspondence address. Tel: +86-21-25076700; Fax: +86-21-64085875; E-mail: drshumingpan@hotmail.com

Received 21 October 2015; Accepted 1 December 2015

Abstract

In this study, we investigated the neuroprotective potential of resveratrol against oxygen glucose deprivation/reoxygenation (OGD/R)-induced apoptotic damages in well-differentiated PC12 cells and the underlying mechanisms. Cells were incubated under normal condition or OGD/R in the presence or absence of 10 μM resveratrol. Cell viability was determined with methyl-thiazolyl-tetrazolium (MTT) assay. Apoptotic ratio was determined with Hoechst 33342 staining and Annexin V-FITC/PI double staining. Oxidative stress was evaluated by measuring the intracellular reactive oxygen species (ROS), the mitochondrial superoxide, the malondialdehyde (MDA) content, and the activities of superoxide dismutase (SOD) and catalase (CAT). The intracellular calcium ($[Ca^{2+}]i$) was estimated by Fluo-3/AM. The mitochondrial membrane potential (MMP) was evaluated by 5,5′,6,6′-tetrachloro-1,1,3,3′-tetraethyl-benzimidazolyl-carbocyanine iodide (JC-1) and rhodamine 123 (Rh123). The opening of mitochondrial permeability transition pore (MPTP) was determined by the Calcein/Co^{2+}-quenching technique. The protein levels of cytochrome c, Bcl-2, Bax, cleaved caspase-9, and cleaved caspase-3 were detected by western blot analysis. The results showed that 10 μM resveratrol attenuated OGD/R-induced cell viability loss and cell apoptosis, which was associated with the decreases in the MDA content and the increases in the SOD and CAT activities. Furthermore, the accumulation of intracellular ROS and mitochondrial superoxide, disturbance of $[Ca^{2+}]i$ homeostasis, reduction of MMP, opening of MPTP, and release of mitochondrial cytochrome c observed in OGD/R-injured cells, which indicated a switch on the mitochondrial-mediated apoptotic pathway, were all reversed by resveratrol. These results suggest that resveratrol administration may play a neuroprotective role via modulating the mitochondrial-mediated signaling pathway in OGD/R-induced PC12 cell injury.

Key words: resveratrol, neuroprotection, oxygen glucose deprivation/reoxygenation, apoptosis, mitochondrial function

Introduction

Ischemic stroke, which is resulted from the acute occlusion of intracranial blood vessels, accounts for ~85% of all cases of stroke [1]. According to the interaction of severity and the duration of the ischemic insult, it is possible to identify a territory, the 'core', which is characterized by an extremely low cerebral blood flow (CBF) and irreversibly necrotic cell death, and a peripheral area, the 'penumbra', which suffers from a moderate reduction in CBF and contains functionally impaired but still salvageable brain tissue [2]. Although the subsequently restored CBF counteracts ischemic injury to some extent,

huge amount of reactive oxygen species (ROS) damages mitochondrial function and triggers a significant activation of signal transduction cascades to cause a disturbance of calcium homeostasis in neuronal cells [3], ultimately resulting in apoptotic cell death [4]. Consequently, reducing oxidative stress may provide a specific therapeutic target for ischemic stroke.

Antioxidant strategies for ischemic stroke have achieved encouraging results in extensive studies. For instance, edaravone that has been used in the treatment of patients with ischemic stroke inhibits both water-soluble and lipid-soluble peroxyl radical-induced peroxidation systems [5]. Resveratrol (trans-3,4′,5-trihydroxystilbene), a unique phytoalexin widely distributed in natural plants, possesses a strong antioxidant activity capable of opposing the potentially cytotoxic stresses of oxidative damage [6]. Several *in vitro* studies have identified that resveratrol may protect various neuronal cell types from oxidative stress-induced cell death [7–9]. A previous *in vivo* research has suggested that dietary administration of resveratrol to elderly male Wistar rats confers protection against recurrent ischemic insult caused by two mild transient middle cerebral artery occlusions [10]. However, whether resveratrol plays a neuroprotective role via the mitochondrial-mediated signaling pathway is still unknown, and the molecular mechanism of resveratrol action has not been sufficiently elucidated.

PC12 is a cell line derived from rat pheochromocytoma and has been widely used as an *in vitro* model for investigating neuronal apoptosis, oxygen sensor mechanism, and neuronal differentiation [11]. In this study, we tested the hypothesis that resveratrol may have neuroprotective potential in oxygen glucose deprivation/reoxygenation (OGD/R)-induced PC12 cell apoptosis through mitochondrial-mediated signaling pathway.

Materials and Methods

Reagents and chemicals

Well-differentiated PC12 cells were purchased from the Cell Resource Center of Shanghai Institutes for Biological Sciences, Chinese Academy of Sciences (Shanghai, China). Dulbecco's modified Eagle's medium (DMEM), fetal bovine serum (FBS), phosphate buffer solution (PBS), Hank's balanced salt solution (containing calcium) (HBSS/Ca^{2+}), and penicillin/streptomycin mixture were from Life Technologies (Grand Island, USA). Resveratrol, dimethylsulfoxide (DMSO), 3-(4,5-dimethylthiazol-2-yl)-2,5-diphenyltetrazolium bromide (MTT), Hoechst 33342, dihydroethidium (DHE), dihydrorhodamine 123 (DHR123), 5,5′,6,6′-tetrachloro-1,1,3,3′-tetraethylbenzimidazolyl-carbocyanine iodide (JC-1), and rhodamine 123 (Rh123) were from Sigma-Aldrich (St Louis, USA). Annexin V-FITC/PI Apoptosis Detection Kit was from BD Biosciences (San Diego, USA). Superoxide dismutase (SOD) Activity Assay Kit was from BioVision (Mountain View, USA). Fluo-3/AM probe was from Biotium (Suite Hayward, USA). MitoSOX™ Red mitochondrial superoxide indicator and MitoProbe Transition Pore Assay Kit were from Molecular Probes (Life Technologies). Cytochrome c Releasing Apoptosis Assay Kit was from Abcam (Cambridge, UK). Rabbit anti-Bcl-2, rabbit anti-Bax, rabbit anti-caspase-9, rabbit anti-caspase-3, and rabbit anti-cytochrome c oxidase subunit IV (COX IV) antibodies were from Cell Signaling Technology (Beverly, USA). Mouse anti-β-actin and horseradish peroxidase-conjugated secondary antibodies were from Beyotime (Beyotime Institute of Biochemistry, Shanghai, China). Enhanced chemiluminescence kit was from Millipore (Billerica, USA). All other chemicals and reagents were of analytical grade.

Cell culture

Well-differentiated PC12 cells were seeded in 25 cm^2 polystyrene flasks with 4.5 g/l glucose in DMEM medium, containing 10% heat-inactivated FBS, 100 U/ml penicillin, and 100 μg/ml streptomycin. Cells were incubated at 37°C under a humidified atmosphere of 95% air and 5% CO_2. Culture medium was replaced every 48 h, and cultures were split at a ratio of 1 : 6 once a week. Prior to experiments, cells were assessed for cell viability by trypan blue dye exclusion test, and only cell batches showing >95% viability were used in the study.

OGD/R model

Well-differentiated PC12 cells were washed with PBS for three times and resuspended in pre-warmed (37°C) DMEM medium that contains all the standard components except glucose. Then cells were allowed to grow in a hypoxia chamber (Thermo scientific, Waltham, USA) with a compact oxygen controller to maintain oxygen concentration at 1% by injecting a gas mixture of 94% N_2 and 5% CO_2 for 6 h. After hypoxia, the cells were then transferred back to normal DMEM medium containing 4.5 g/l glucose under an atmosphere of 95% air and 5% CO_2, and incubated for 24 h for reoxygenation [8].

Study groups

Biologically safe doses of resveratrol were determined prior to application. PC12 cells were exposed to increasing concentrations (2.5–40 μM) of resveratrol for 24 h. MTT assay was subsequently performed, and 10 μM resveratrol was selected for the further mechanistic study, because higher concentrations of resveratrol decreased cell viability. Four experimental groups were assigned: (i) control, (ii) resveratrol, (iii) OGD/R, and (iv) OGD/R + resveratrol. In the OGD/R + resveratrol group, resveratrol was added to the culture media 1 h prior to the OGD/R.

MTT assay and morphological observation for the determination of cell viability

MTT assay was performed following the protocols of Agrawal *et al.* [8] with some modification. In brief, cells (1×10^4) were seeded in 96-well microculture plates that had been pre-coated poly-L-lysine and cultured overnight in complete DMEM medium in a CO_2 incubator (95% air/5% CO_2). Subsequently, cells were treated with resveratrol (2.5, 5, 10, 20, and 40 μM) alone for 24 h to evaluate the cytotoxicity of resveratrol. For neuroprotective potential of resveratrol against OGD/R neurotoxicity study, resveratrol (2.5, 5, 10, and 20 μM) was added to the cultures 1 h prior to the OGD/R. The treated cells were visualized using a Leica DMI-3000B phase-contrast fluorescence microscope (Leica, Heidelberg, Germany) equipped with a digital camera. Then, cells were incubated in a serum-free medium containing MTT solution in the darkness for 4 h at 37°C. The MTT solution was discarded, and 100 μl DMSO was added to each well to dissolve the formazan crystals. The value of optical density was measured at wave length of 562 nm using a Bio-Rad microplate reader (Bio-Rad, Hercules, USA). Cell survival for each treatment was calculated as a percentage of the control.

Detection of apoptotic ratio

To evaluate the effect of resveratrol on OGD/R-induced apoptosis, Hoechst 33342 staining assay was performed. Cells were incubated in the presence of 10 μg/ml Hoechst 33342 in the dark for 15 min at 37°C and then washed three times with PBS. The fluorescence was observed using a Leica DMI-3000B phase-contrast fluorescence microscope (Leica).

For quantitative analysis, apoptotic ratio was assessed using the Annexin V-FITC/PI Apoptosis Detection Kit following the manufacturer's instructions. Cells were trypsinized, harvested, washed with PBS for three times, resuspended in 100 μl binding buffer at a concentration of 1×10^6 cells/ml, and then incubated with a combination of 5 μl FITC Annexin V and 5 μl PI working solution for 15 min in the dark at room temperature. FITC and PI fluorescence were measured using a flow cytometer (BD Bioscience) with an excitation wavelength of 488 nm and an emission wavelength of 530 nm. At least 1×10^5 events were recorded. After the quadrants on the Annexin V/PI dot plots were positioned, live cells (Annexin V^-/PI^-), early/primary apoptotic cells (AnnexinV^+/PI^-), late/secondary apoptotic cells (Annexin V^+/PI^+), and necrotic cells (Annexin V^-/PI^+) were distinguished.

Detection of intracellular ROS production

The intracellular ROS production was assessed using the DHE probe. Cells were incubated in the presence of 10 μM DHE in the dark for 1 h at 37°C and then washed three times with PBS. The fluorescence was observed using a Leica DMI-3000B phase-contrast fluorescence microscope (Leica) with 520 nm excitation and 610 nm emission.

For quantitative analysis, DHR123 probe was used as an intracellular ROS capture. Briefly, PC12 cells (5×10^5) were washed with PBS for three times and then incubated with 5 μM DHR123 in the dark for 1 h at 37°C. Cells were trypsinized, harvested, washed three times with PBS, and directly resuspended in PBS before an immediate detection of mean fluorescence intensity (MFI) of DHR123 using a flow cytometer (BD Bioscience) with 488 nm excitation and 525 nm emission, and at least 1×10^4 events per sample were acquired.

Detection of mitochondrial superoxide generation

The mitochondrial superoxide generation was monitored using the MitoSOX™ Red indicator according to the manufacturer's instructions. Cells were incubated with 5 μM MitoSOX™ reagent working solution in the dark for 10 min at 37°C and then washed three times with HBSS. The fluorescence was observed using a phase-contrast fluorescence microscope with 510 nm excitation and 580 nm emission.

For quantitative analysis, PC12 cells (1×10^6) were washed with HBSS for three times and then incubated with 5 μM MitoSOX™ reagent working solution in the dark for 10 min at 37°C. Cells were trypsinized, harvested, washed three times with HBSS, and directly resuspended in HBSS before an immediate detection of MFI of MitoSOX™ by a flow cytometer with 510 nm excitation and 580 nm emission, and at least 1×10^4 events per sample were acquired.

Detection of lipid peroxidation

The malondialdehyde (MDA) content of PC12 cells in each group was detected to assess the levels of membrane lipid peroxidation as previously described [12]. Briefly, 100 μl supernatant was collected and mixed with 1.5 ml acetic acid (20%), 1.5 ml thiobarbituric acid (0.8%), and 200 μl sodium dodecyl sulphate (SDS) (8%). Each reaction mixture was heated for 1 h at 95°C and cooled to room temperature. Then, 5 ml of *n*-butanol was added. After mixing and centrifugation at 3000 *g* for 10 min, the organic layer was collected and the absorbance was measured at the wave length of 532 nm.

Detection of antioxidant enzyme activity

To assess the levels of endogenous antioxidant, superoxide dismutase (SOD) and catalase (CAT) activities of PC12 cells in each group were detected. The SOD activity was determined using the SOD Activity Assay Kit following the manufacturer's protocol. Briefly, 20 μl supernatant was mixed with 200 μl tetrazolium working solution and 20 μl enzyme working solution. After 20 min of incubation at 37°C, the absorbance was read at 450 nm. The CAT activity was estimated according to the instructions of Shen *et al.* [13] with some modification. Briefly, 1 ml hydrogen peroxide (10%) was added to 50 μl supernatant diluted in 1.95 ml PBS. The CAT activity was then quantified from the decrease in absorbency at 240 nm for 2 min.

Detection of intracellular calcium ($[Ca^{2+}]i$)

The concentration of $[Ca^{2+}]i$ was measured with Fluo-3/AM probe [14]. Cells were incubated with 5 μM Fluo-3/AM in the dark for 30 min at 37°C, and then the fluid was removed and cells were washed three times with PBS to remove the nonspecific staining. The treated cells were observed using a phase-contrast fluorescence microscope with 488 nm excitation and 525 nm emission.

For quantitative analysis, PC12 cells (5×10^5) were washed with PBS for three times and then incubated with 5 μM Fluo-3/AM in the dark for 30 min at 37°C. Cells were trypsinized, harvested, washed three times with PBS, and directly resuspended in PBS before an immediate detection of MFI of Fluo-3/AM by a flow cytometer with 488 nm excitation and 525 nm emission, and at least 5×10^4 events per sample were acquired.

Detection of mitochondrial membrane potential

The mitochondrial membrane potential (MMP) was assessed using the JC-1 probe. JC-1 exists as a green fluorescent monomer at low MMP, while at higher MMP, JC-1 forms red fluorescent aggregates and can therefore be used as a sensitive measure of changes in MMP. After being incubated with 10 μg/ml JC-1 in the dark for 20 min at 37°C, cells were washed with PBS for three times and subject to laser scanning confocal microscope analysis (Zeiss LSM510; Zeiss, Oberkochen, Germany). JC-1-loaded cells were excited at 488 nm, and emission was detected at 590 nm (JC-1 aggregates) and 525 nm (JC-1 monomers).

For quantitative analysis, MMP was also measured using the cell permeable cationic fluorescence probe Rh123. PC12 cells (5×10^5) were washed with PBS for three times and then incubated with 1 μM Rh123 in the dark for 30 min at 37°C. Then cells were trypsinized, harvested, washed three times with PBS, and directly resuspended in PBS. MFI of Rh123-labeled cells was analyzed by a flow cytometer with 488 nm excitation and 525 nm emission, and at least 1×10^4 events per sample were acquired.

Detection of mitochondrial permeability transition pore opening

The opening of the mitochondrial permeability transition pore (MPTP) was determined by the Calcein/Co^{2+}-quenching technique via the MitoProbe Transition Pore Assay Kit (Life Technologies) according to the manufacturer's instructions. Cells were incubated with 1 μM Calcein/AM and in the presence of 1 mM cobalt chloride ($CoCl_2$) in the dark for 15 min at 37°C and then were washed three times with HBSS. The fluorescence was observed via a phase-contrast fluorescence microscope with 494 nm excitation and 517 nm emission.

For quantitative analysis, PC12 cells (1×10^6) were washed with HBSS for three times and then incubated with 1 μM Calcein/AM and 1 mM $CoCl_2$ in the dark for 15 min at 37°C. Cells were trypsinized, harvested, washed three times with HBSS, and directly resuspended in HBSS before an immediate detection of MFI of Calcein/AM by a flow cytometer with 494 nm excitation and 517 nm emission, and at least 1×10^4 events per sample were acquired.

Cytochrome c release assay

Cytochrome c release was measured by using the Cytochrome c Releasing Apoptosis Assay Kit (Abcam). Briefly, cells were collected

by centrifugation and washed twice with PBS. Cells were homogenized and subject to cytosolic and mitochondrial extraction by employing the corresponding reagents. Then, 30 μg of protein sample from each of the cytosolic or mitochondrial fraction was subject to 12% sodium dodecyl sulfate–polyacrylamide gel electrophoresis (SDS–PAGE). A standard western blot analysis procedure was done and probed with monoclonal mouse anti-cytochrome c antibody. Mouse anti-β-actin and rabbit anti-COX IV antibodies were used as internal controls for the cytosolic fraction and the mitochondrial fractions, respectively. Data were analyzed by Science Lab 2005 Image Gauge software.

Western blot analysis

Cellular proteins were lysed in Radio Immunoprecipitation Assay buffer and then centrifuged at 10,000 *g* for 15 min at 4°C. Equal amounts of protein samples (50 μg) were loaded per lane and resolved by 15% SDS/PAGE. Then, proteins were electrotransferred onto a polyvinylidene fluoride (PVDF) membrane. The membranes were blocked with 5% nonfat milk for 1 h at room temperature and then incubated with rabbit anti-Bcl-2 (1:1000, Cell Signaling Technology), rabbit anti-Bax (1:1000, Cell Signaling Technology), rabbit anti-caspase-9 (1:1000, Cell Signaling Technology), rabbit anti-caspase-3 (1:1000, Cell Signaling Technology), and mouse anti-β-actin (1:1000, Beyotime Institute of Biochemistry) antibodies separately overnight at 4°C. After being washed three times with Tris buffered saline containing 0.1% Tween-20, the membranes were incubated with the corresponding HRP-conjugated secondary antibody (1:1000, Beyotime Institute of Biochemistry) in blocking solution at room temperature for 2 h. The signals of bound antibodies were identified with an enhanced chemiluminescence kit (Millipore). The band intensity was measured, normalized by β-actin, and calculated as the ratio of the optical density. Data were analyzed by Science Lab 2005 Image Gauge software.

Statistical analysis

Reproducibility of the results was ensured by repeating all experiments at least three times. Data were presented as mean ± standard deviation (SD). Statistical significance was determined by one-way ANOVA followed by Tukey's *post hoc* test. $P < 0.05$ was considered significant.

Results

Resveratrol inhibited OGD/R-induced cell viability loss

To determine the biologically safe concentrations of resveratrol, cells were exposed to resveratrol with increasing concentrations from 2.5 to 40 μM for 24 h (**Fig. 1A**). The MTT assay revealed that PC12 cells treated with 20 μM or lower concentrations of resveratrol were found to be almost 100% viable, which demonstrated that resveratrol with varying concentrations from 2.5 to 20 μM did not induce any significant cell viability loss. However, higher concentration of resveratrol (40 μM) decreased cell viability (86.00% ± 4.23% of control value, $P < 0.05$ vs. control), indicating that resveratrol over 40 μM is deleterious to neuronal cells.

Furthermore, OGD/R-injured PC12 cells were treated with biologically safe doses of resveratrol (2.5, 5, 10, and 20 μM). Our data showed that cell viability decreased prominently after OGD/R insult (63.80% ± 2.23% of control value, $P < 0.01$ vs. control). Improvements in cell viability were observed in 2.5, 5, 10, and 20 μM resveratrol groups (73.09% ± 4.12%, 81.13% ± 4.24%, 87.80% ± 3.39%, and 72.55% ± 3.46% of control value, respectively) with its maximum protective effect at 10 μM, compared with the OGD/R group (**Fig. 1B**).

Cellular morphology was observed under a phase-contrast fluorescence microscope (**Fig. 1C**). Normal neuronal morphology was observed in the control group and 10 μM resveratrol group, showing cone shape or multipolarity with regular contours. After OGD/R insult, the number of PC12 cells showed a significant reduction, and the morphology exhibited round, slender and degenerated with cell debris. When OGD/R-injured cells were incubated with 10 μM resveratrol, the number of cells increased dramatically and normal morphology was restored. These observations were in accordance with the results of MTT assay.

These results indicated that 10 μM resveratrol is the optimal dose for its neuroprotective effects on OGD/R-induced cytotoxicity in PC12 cells. Thus, 10 μM resveratrol was selected for further mechanistic study.

Resveratrol prevented OGD/R-induced apoptosis

Apoptosis after cerebral ischemia/reperfusion is one of the major pathways that lead to the process of cell death [4]. Therefore, we investigated the anti-apoptotic effects of 10 μM resveratrol using Hoechst 33342 staining assay, which could qualitatively distinguish apoptotic cells from normal cells based on nuclear condensation and fragmentation. **Figure 1D** showed that the control group and resveratrol group did not exhibit brightly stained condensed nuclei, suggesting no or minimum apoptosis. On the contrary, most cells in the OGD/R group showed typical characteristics of apoptosis, including the condensed and fragmented nuclei, and the appearance of a few apoptotic bodies. Treatment with 10 μM resveratrol partially recovered the abnormal morphological changes of apoptosis induced by OGD/R.

To provide further evidence that resveratrol prevents OGD/R-induced apoptosis, flow cytometry with Annexin V-FITC/PI double staining was performed. As shown in **Fig. 1E,F**, the percentages of apoptotic cells in the control group and resveratrol group were 4.35% ± 0.50% and 3.65% ± 0.92% ($P > 0.05$), respectively, indicating that 10 μM resveratrol alone did not change the apoptotic ratio compared with the control. However, the apoptotic ratio was as high as 20.90% ± 1.27% after OGD/R insult ($P < 0.01$ vs. control) and markedly decreased to 8.15% ± 0.50% in OGD/R + resveratrol group ($P < 0.01$ vs. OGD/R), indicating that 10 μM resveratrol can effectively prevent OGD/R-induced apoptosis.

Resveratrol attenuated OGD/R-induced intracellular ROS accumulation

Intracellular ROS production was observed by a phase-contrast fluorescence microscope using the fluorescent probe DHE (**Fig. 2A**). Normal PC12 cells exhibited weak red fluorescence in the control group and resveratrol group, whereas OGD/R-injured PC12 cells presented enhanced red fluorescence, implying ROS accumulation in the injured cells. After treatment with 10 μM resveratrol, the intensity of the red fluorescence was dramatically reduced.

Furthermore, we measured the level of DHR123 fluorescence by flow cytometry to quantify the level of intracellular ROS. When PC12 cells were exposed to OGD/R, MFI of the intracellular ROS was increased from 691.03 ± 70.71 (the control group) to 1086.51 ± 64.35 (the OGD/R group) ($P < 0.05$), revealing that OGD/R enhanced the levels of ROS in PC12 cells. Conversely, treatment with 10 μM resveratrol effectively reduced OGD/R-induced ROS production to 740.54 ± 84.15 ($P < 0.05$ vs. OGD/R) (**Fig. 2B,C**).

Resveratrol attenuated OGD/R-induced mitochondrial superoxide accumulation

Mitochondria are the major source of superoxide which is the main component of oxidative stress [15]. To investigate the contribution

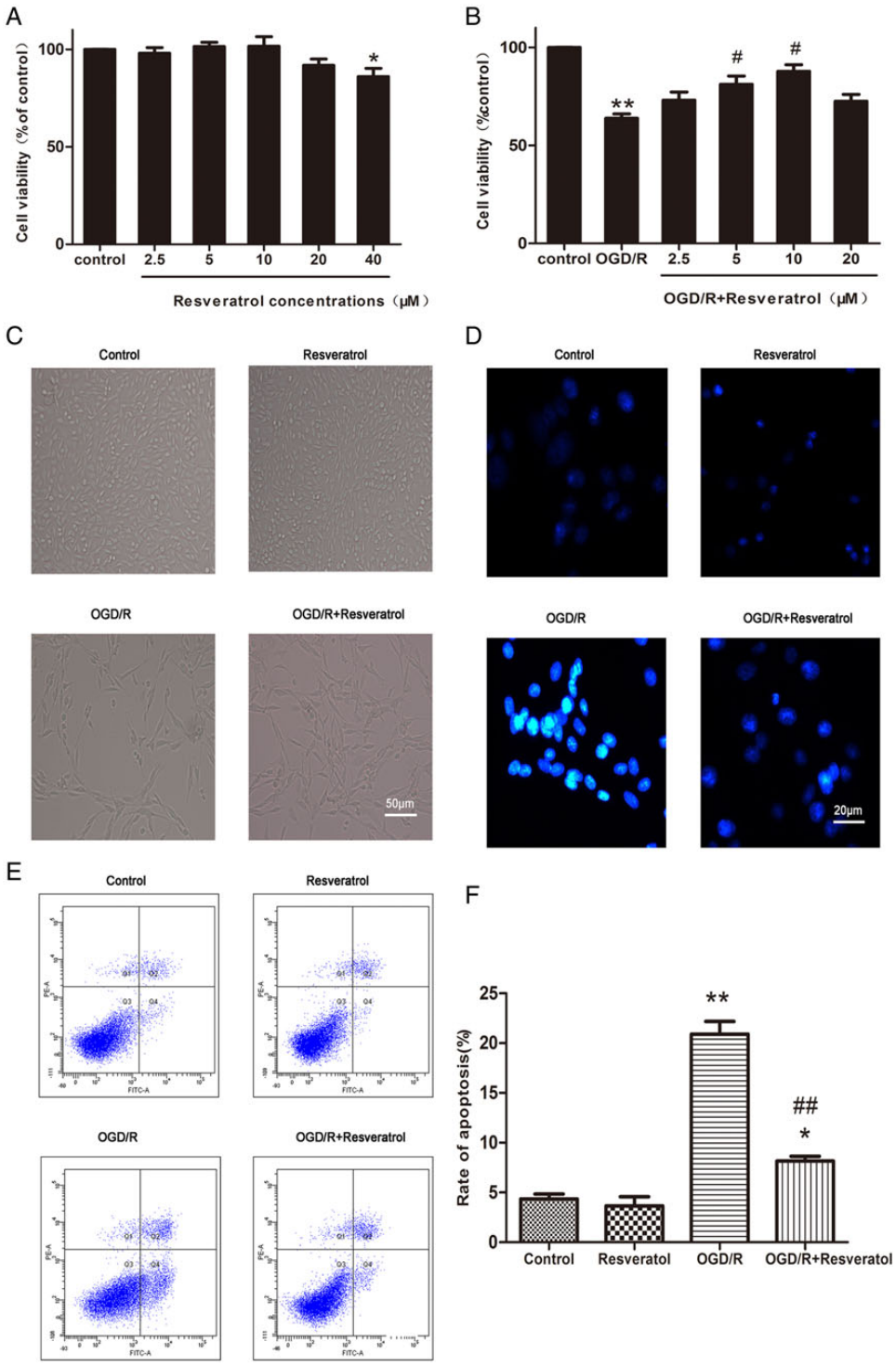

Figure 1. Resveratrol inhibited OGD/R-induced cell viability loss and cell apoptosis (A) MTT assay showed that resveratrol (2.5–20 μM) were safe for PC12 cells, only higher concentration (40 μM) decreased cell viability. Values obtained from three independent experiments are expressed as mean ± SD (% of control). (B) Protective potential of resveratrol (2.5–20 μM) on cell viability in PC12 cells exposed to OGD/R. Representative phase-contrast (C) and fluorescence (D) images showed that decreased PC12 cells exposed to OGD/R were restored by 10 μM resveratrol. Scale bar represents 50 μm in C and 20 μm in D. Flow cytometer images (E) and quantification (F) showed that OGD/R-induced PC12 cell apoptosis was rescued by 10 μM resveratrol. $^{*}P<0.05$ vs. control; $^{**}P<0.01$ vs. control; $^{\#}P<0.05$ vs. OGD/R; $^{\#\#}P<0.01$ vs. OGD/R.

of mitochondria to OGD/R-induced ROS production, mitochondrial superoxide generation was measured using MitoSOX™ Red indicator, which served as a novel fluorescent probe for highly selective detection of superoxide in the mitochondria of live cells. Previous evidence has demonstrated that MitoSOX™ reagent is oxidized by superoxide and exhibits red fluorescence once in the mitochondria [15]. As

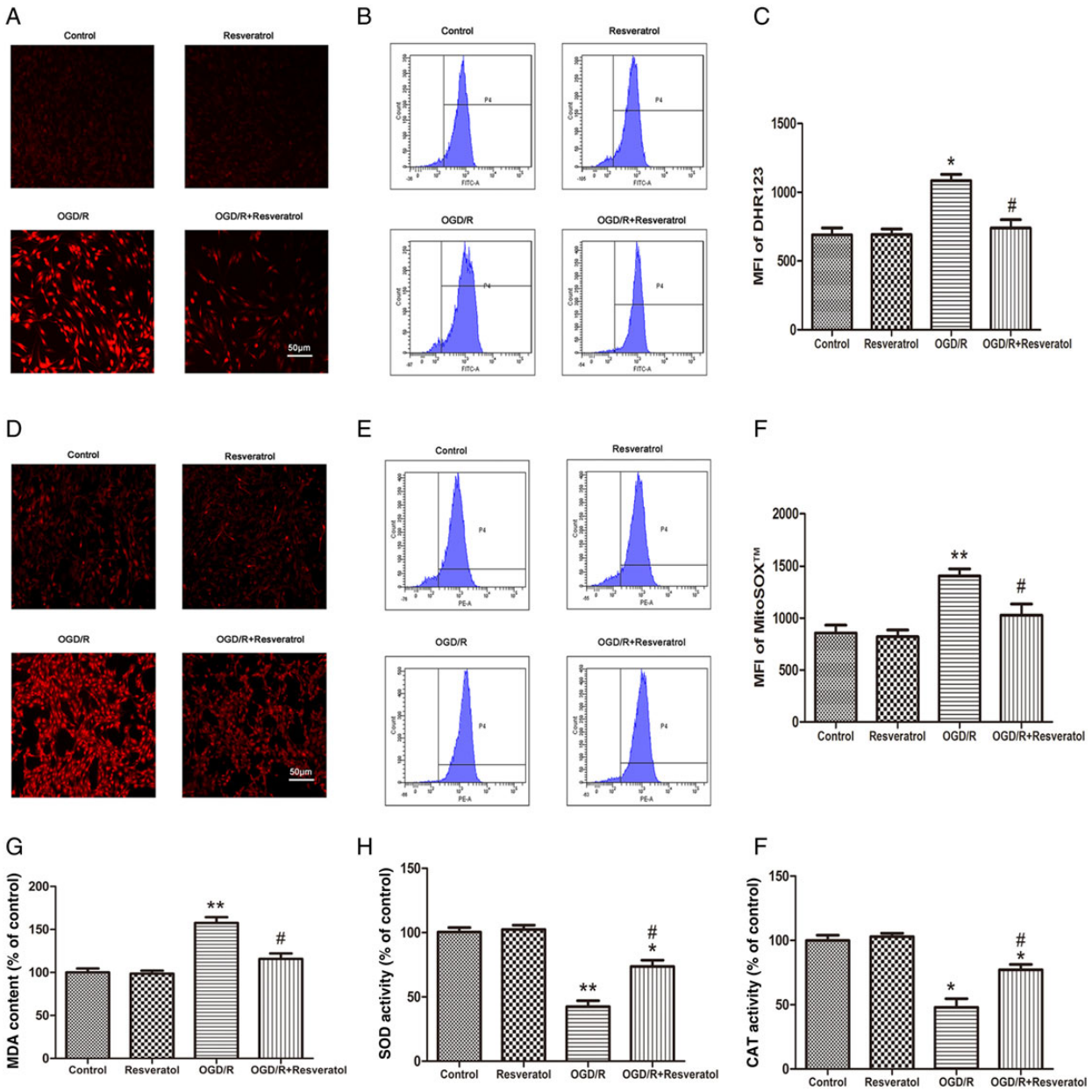

Figure 2. Resveratrol attenuated OGD/R-induced oxidative stress (A) Representative fluorescence images of intracellular ROS observed with DHE probe. Scale bar represents 50 μm. Flow cytometry images (B) and quantification (C) of DHR123 probe showed that OGD/R-induced intracellular ROS accumulation was rescued by 10 μM resveratrol. (D) Representative fluorescence images of mitochondrial superoxide observed with MitoSOX™ probe. Scale bar represents 50 μm. Flow cytometer images (E) and quantification (F) of MitoSOX™ probe showed that OGD/R-induced mitochondrial superoxide accumulation was rescued by 10 μM resveratrol. Lipid peroxidation was evaluated by measuring MDA content (G), and antioxidant enzyme activity by measuring activities of SOD (H) and CAT (I). Results showed that 10 μM resveratrol reversed OGD/R-induced increase in MDA content and decrease in SOD and CAT activities. Values obtained from three independent experiments are expressed as mean ± SD.* $P < 0.05$ vs. control;** $P < 0.01$ vs. control; # $P < 0.05$ vs. OGD/R.

shown in **Fig. 2D**, normal PC12 cells exhibited weak red fluorescence in the control group and resveratrol group, while OGD/R-injured PC12 cells presented significantly increased red fluorescence, indicating an increase in mitochondrial superoxide generation. However, treatment with 10 μM resveratrol strongly inhibited OGD/R-induced mitochondrial superoxide accumulation as evidenced by a lower MitoSOX™ fluorescence signal.

Additionally, we measured levels of MitoSOX™ fluorescence by flow cytometry to quantify the levels of mitochondrial superoxide. When PC12 cells were exposed to OGD/R, MFI of the MitoSOX™ was increased in the OGD/R group (1406.67 ± 117.82) compared with the control group (857.31 ± 130.12) ($P < 0.01$), revealing that OGD/R enhanced the levels of mitochondrial superoxide in PC12 cells. Importantly, treatment with 10 μM resveratrol effectively attenuated OGD/R-induced mitochondrial superoxide generation (1029.06 ± 185.82, $P < 0.05$ vs. OGD/R) (**Fig. 2E,F**).

Resveratrol antagonized OGD/R-induced lipid peroxidation

MDA, a by-product of membrane lipid peroxidation, is produced under oxidative stress and reflects oxidative damage of the plasma

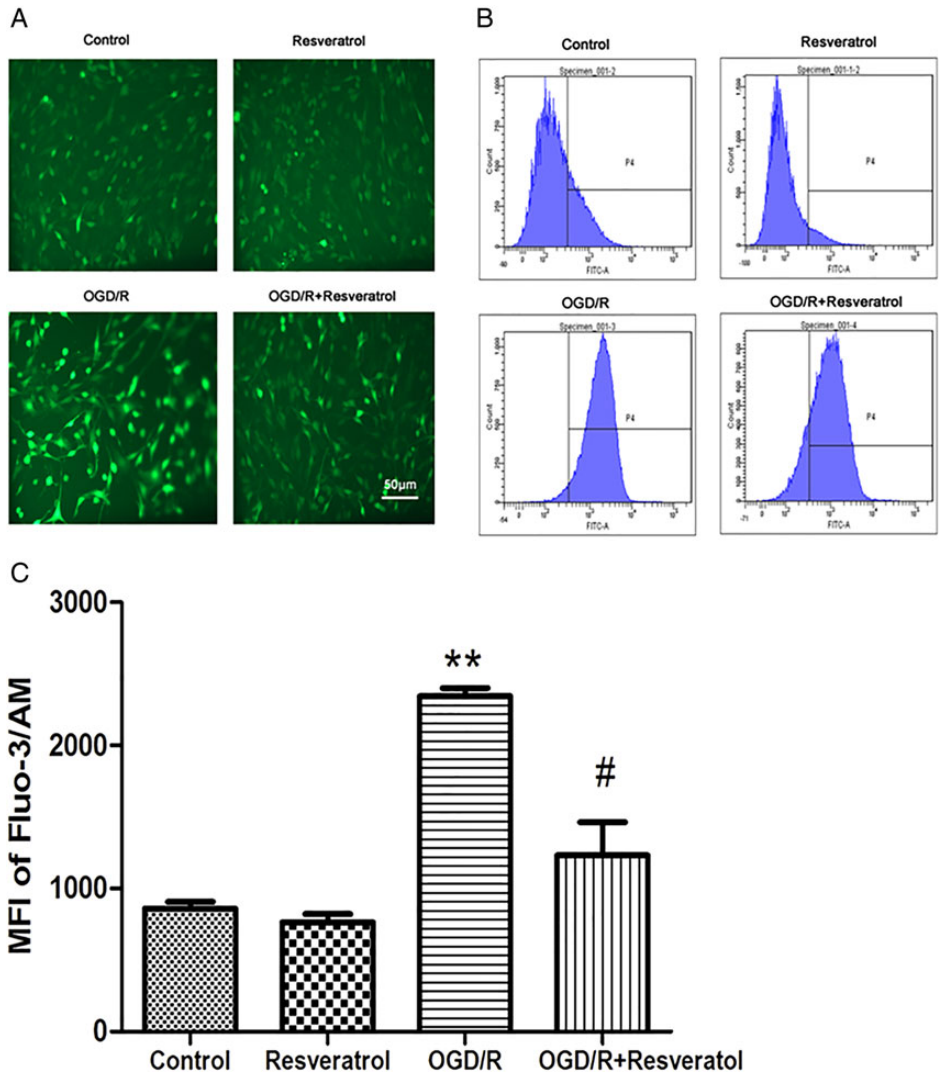

Figure 3. Resveratrol suppressed OGD/R-induced overload of $[Ca^{2+}]i$ (A) Representative fluorescence images of $[Ca^{2+}]i$ observed with Fluo-3/AM probe. Scale bar represents 50 μm. Flow cytometry images (B) and quantification (C) of Fluo-3/AM probe showed that OGD/R-induced overload of $[Ca^{2+}]i$ was rescued by 10 μM resveratrol. Values obtained from three independent experiments are expressed as mean ± SD. $^{**}P < 0.01$ vs. control; $^{\#}P < 0.05$ vs. OGD/R.

membrane [16]. As shown in **Fig. 2G**, the MDA content in the OGD/R group was notably increased to 157.62% ± 6.65% of control value ($P < 0.01$ vs. control), suggesting that OGD/R induced membrane lipid peroxidation in PC12 cells. When OGD/R-injured cells were incubated with 10 μM resveratrol, MDA content (115.84% ± 6.36% of control value) was significantly decreased compared with the OGD/R group ($P < 0.05$ vs. OGD/R).

Resveratrol alleviated OGD/R-induced antioxidant enzyme activity reduction

The SOD activity (**Fig. 2H**) and CAT activity (**Fig. 2I**) were measured to investigate the antioxidant defense systems in PC12 cells for scavenging ROS to prevent OGD/R-induced oxidative damage. It was found that OGD/R insult markedly decreased the SOD and CAT activities (42.40% ± 4.63% and 47.93% ± 6.75% of control value, respectively) ($P < 0.01$ vs. control), indicating that antioxidant enzyme activities were decreased in PC12 cells treated with OGD/R. After treatment with10 μM resveratrol, the SOD and CAT activities were significantly increased (73.68% ± 4.87% and 77.18% ± 4.16% of control value, respectively) ($P < 0.05$ vs. OGD/R).

Resveratrol suppressed OGD/R-induced overload of $[Ca^{2+}]i$

Increase in $[Ca^{2+}]i$ after oxidative insults has been linked to free radical generation, which leads to cell death [3]. To investigate the role of resveratrol on $[Ca^{2+}]i$ during OGD/R, we monitored the levels of $[Ca^{2+}]i$ with the fluorescent probe Fluo-3/AM using a phase-contrast fluorescence microscope (**Fig. 3A**). Green fluorescence detected was rather week in the control group and resveratrol group, and became much stronger in the OGD/R group. Treatment with 10 μM resveratrol prevented the increase of fluorescence induced by OGD/R.

Quantitatively, the OGD/R group showed a significant increase in $[Ca^{2+}]i$ (2344.32 ± 79.90) compared with the control group (857.52 ± 67.18) ($P < 0.01$). However, treatment with 10 μM resveratrol showed a significant reduction in $[Ca^{2+}]i$ (1232.71 ± 327.46, $P < 0.05$ vs. OGD/R) (**Fig. 3B,C**).

Resveratrol ameliorated OGD/R-induced MMP dissipation

To explore the effect of resveratrol on MMP during OGD/R, we determined the changes in MMP with the fluorescent probe JC-1 using a

laser scanning confocal microscope. At high membrane potentials, JC-1 enters the mitochondria and forms aggregates that have a fluorescence of bright red, whereas JC-1 exists as a green fluorescence at a low potential [17]. Therefore, we used the ratio of red/green fluorescence to evaluate the levels of MMP in different groups. As shown in **Fig. 4A**, normal cells exhibited mainly red fluorescence with rather feeble green fluorescence in the control group and resveratrol group. However, OGD/R-injured PC12 cells showed markedly enhanced green fluorescence and slightly increased red fluorescence. The degree of increase in green fluorescence was greater than red fluorescence, revealing a decline in the ratio of red/green fluorescence in the injured cells. After treatment with 10 μM resveratrol, the green fluorescence was decreased significantly, and the ratio of red/green fluorescence was increased compared with the OGD/R group, demonstrating an increase in MMP.

Moreover, we measured levels of Rh123 fluorescence by flow cytometry to quantify the levels of MMP. PC12 cells exposed to OGD/R resulted in a significant decrease in the level of Rh123 fluorescence (10128.38 ± 1595.44) compared with the control (26636.83 ± 1929.17) ($P < 0.05$), indicating that mitochondrial membrane depolarization occurred. Treatment with 10 μM resveratrol (17280.83 ± 1019.42) significantly ameliorated the dissipation of MMP induced by OGD/R ($P < 0.05$ vs. OGD/R), suggesting a role of resveratrol in ameliorating mitochondrial membrane depolarization induced by OGD/R (**Fig. 4B,C**).

Resveratrol blocked OGD/R-induced MPTP opening

To investigate whether the MPTP opening is involved in OGD/R-induced mitochondrial dysfunction and in the effect of resveratrol, we employed Calcein/Co^{2+}-quenching method using a phase-contrast fluorescence microscope. Under normal condition, Calcein/AM selectively localizes in the mitochondria and exhibits green fluorescence; when MPTP opens unusually, the profound release of Calcein/AM to the cytosol is quenched by $CoCl_2$, inducing subsequent loss of green fluorescence [18]. As shown in **Fig. 5A**, normal PC12 cells exhibited strong green fluorescence in the control group and resveratrol group, whereas OGD/R caused a significant decrease in green fluorescence, consistent with MPTP opening in the injured cells. After treatment with 10 μM resveratrol, an intensive green fluorescence was observed, suggesting that 10 μM resveratrol markedly induced the closure of the MPTP.

Furthermore, we measured levels of Calcein/AM fluorescence by flow cytometry to quantify the levels of MPTP opening. Compared with the control group (662.45 ± 29.83), cells in the OGD/R group showed a significantly lower level of green fluorescence (351.04 ± 46.92) ($P < 0.01$). Treatment with 10 μM resveratrol markedly increased Calcein/AM fluorescence intensity (568.37 ± 27.03, $P < 0.01$ vs. OGD/R); however, the fluorescence intensity could not be restored completely ($P < 0.05$ vs. control) (**Fig. 5B,C**).

Resveratrol inhibited OGD/R-induced cytochrome c release from mitochondria

Release of cytochrome c from mitochondria to cytosol is considered as a key initial step in the mitochondrial-mediated apoptosis pathway. We examined the levels of cytochrome c in cytosol and mitochondria by western blot analysis. Compared with the control group, the OGD/

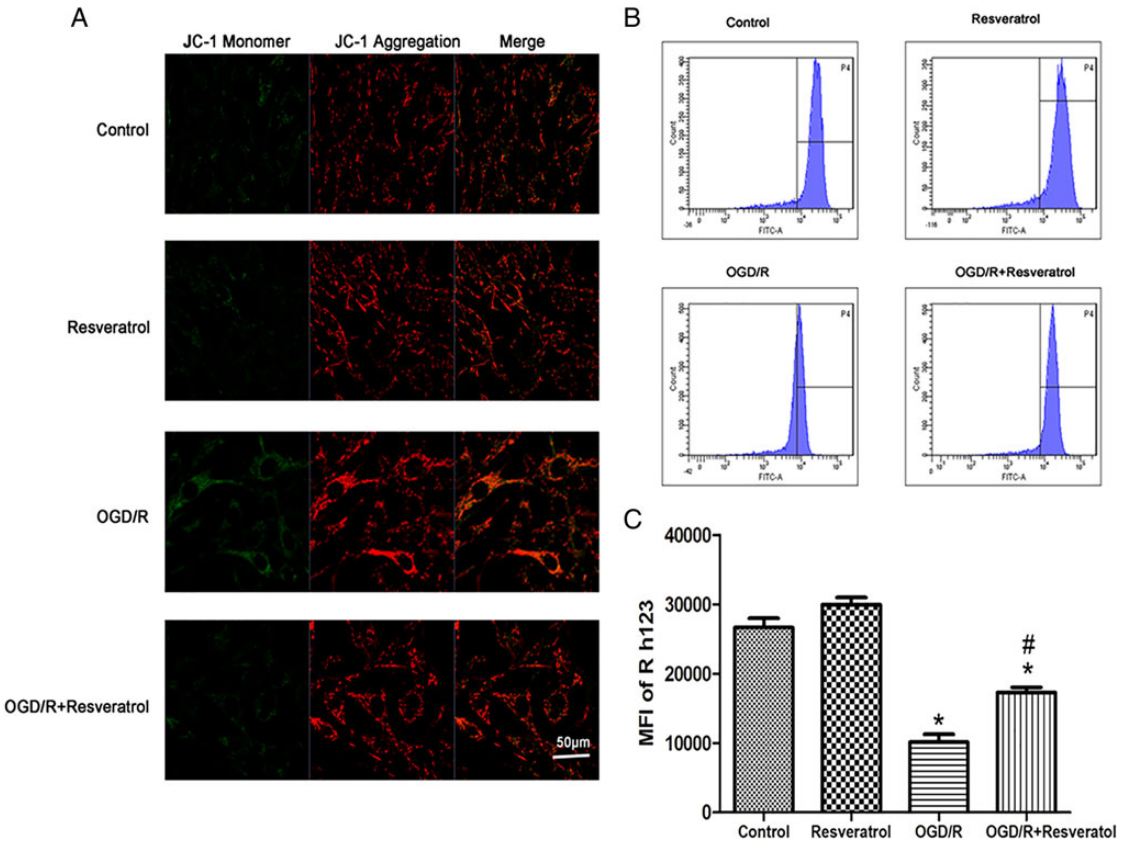

Figure 4. Resveratrol ameliorated OGD/R-induced MMP dissipation (A) Representative fluorescence images of MMP observed with JC-1 probe. Scale bar represents 50 μm. Flow cytometry images (B) and quantification (C) of Rh123 probe showed that OGD/R-induced MMP dissipation was rescued by 10 μM resveratrol. Values obtained from three independent experiments are expressed as mean ± SD. *$P < 0.05$ vs. control; #$P < 0.05$ vs. OGD/R.

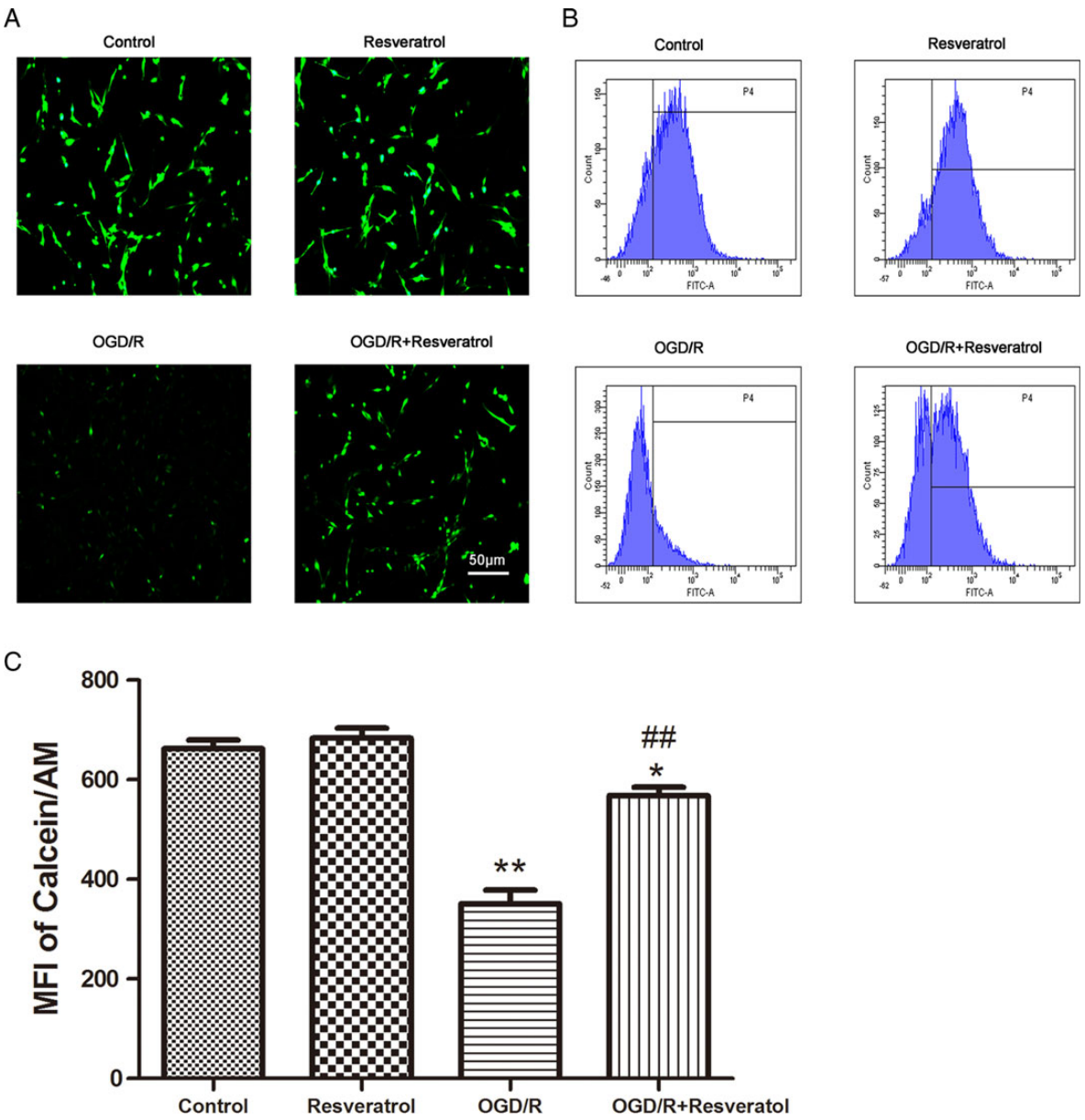

Figure 5. Resveratrol blocked OGD/R-induced MPTP opening (A) Representative fluorescence images of MPTP observed with Calcein/AM probe. Scale bar represents 50 μm. Flow cytometry images (B) and quantification (C) of Calcein/AM probe showed that OGD/R-induced MPTP opening was rescued by 10 μM resveratrol. Values obtained from three independent experiments are expressed as mean ± SD. $^{*}P < 0.05$ vs. control; $^{**}P < 0.01$ vs. control; $^{\#\#}P < 0.01$ vs. OGD/R.

R group showed higher protein levels of cytochrome c in cytosol ($P < 0.01$). In contrast, cells treated with 5 or 10 μM resveratrol showed lower protein levels of cytochrome c in cytosol than OGD/R-injured cells in a dose-dependent manner. Cells treated with 5 or 10 μM resveratrol alone did not show any significant decrease compared with the control ($P > 0.05$ vs. control) (**Fig. 6A,B**).

On the other hand, the OGD/R group showed significantly decreased protein levels of cytochrome c in mitochondria compared with the control group ($P < 0.05$). Conversely, cells treated with 5 or 10 μM resveratrol showed higher protein levels of cytochrome c in mitochondria than the OGD/R-injured cells in a dose-dependent manner. Cells treated with 5 or 10 μM resveratrol alone did not show any difference compared with the control ($P > 0.05$ vs. control) (**Fig. 6C,D**).

Resveratrol increased the ratio of Bcl-2/Bax and decreased protein levels of cleaved caspase-9 and cleaved caspase-3

Because the loss of MMP and opening of MPTP were observed in the OGD/R-injured PC12 cells, we further investigated whether the mitochondrial dysfunction was mediated by the downregulation of Bcl-2 and the upregulation of Bax. The balance between Bcl-2 and Bax is critical in the activation of terminal caspases such as caspase-9 and caspase-3 [19]. Treatment of PC12 cells with OGD/R significantly decreased protein levels of Bcl-2 and increased protein levels of Bax compared with the control group, which resulted in a low ratio of Bcl-2/Bax ($P < 0.05$ vs. control) (**Fig. 6E,F**) and subsequently increased protein levels of cleaved caspase-9 ($P < 0.01$ vs. control) (**Fig. 6G,H**) and

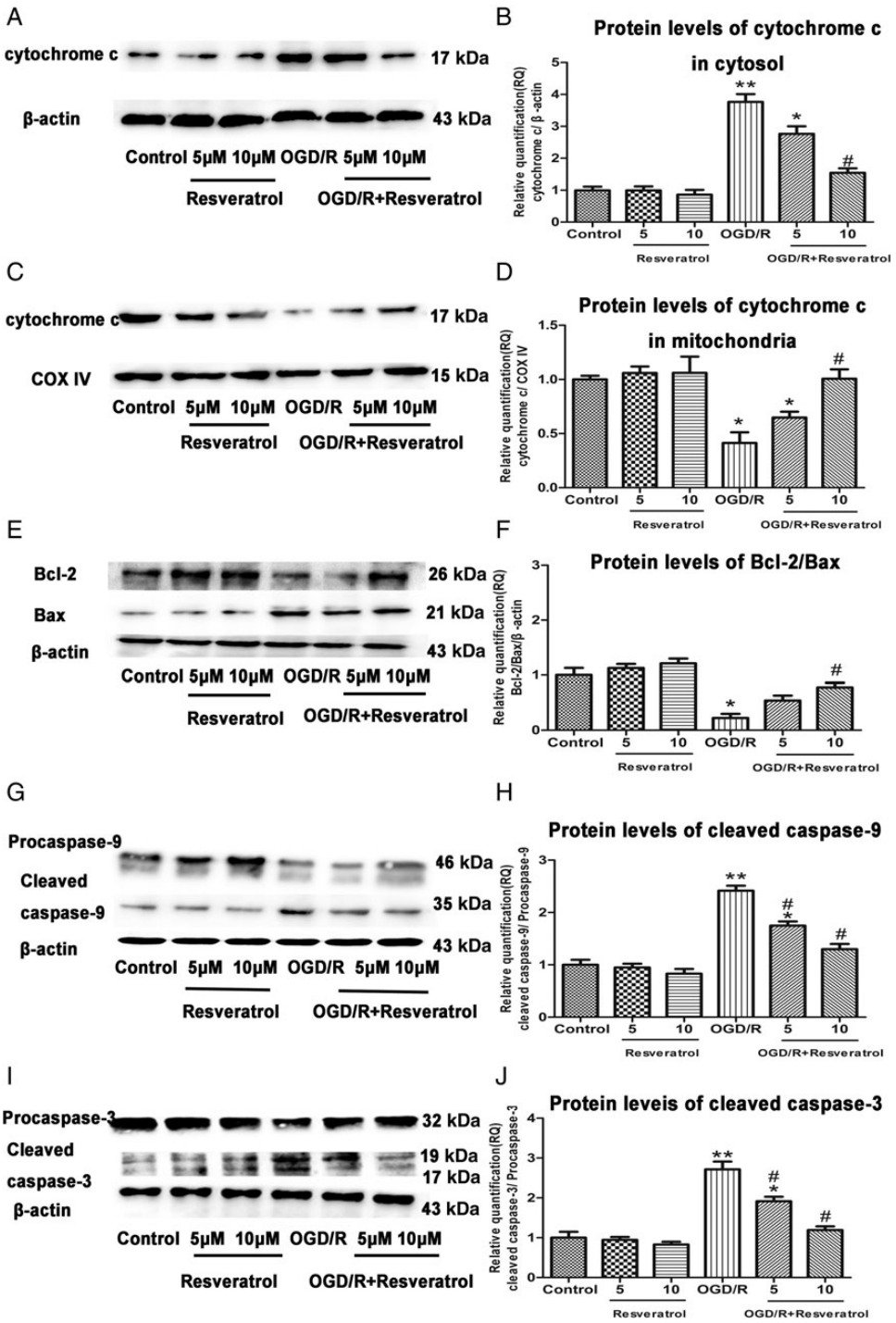

Figure 6. Resveratrol inhibited OGD/R-induced mitochondrial cytochrome c release, decrease of Bcl-2/Bax ratio, and increase of cleaved caspase-9 and cleaved caspase-3 The protein levels of cytochrome c in cytosol (A) and in mitochondria (C) were detected by western blot analysis. β-Actin and COX IV levels were measured to ensure equal protein loading. Relative quantification (RQ) analyses of the induction in the protein levels of cytochrome c in cytosol (B) and in mitochondria (D) showed that 10 μM resveratrol inhibited OGD/R-induced cytochrome c release from mitochondria to cytosol in a dose-dependent manner. The protein levels of Bcl-2, Bax (E), cleaved caspase-9 (G), and cleaved caspase-3 (I) were detected by western blot analysis. β-Actin levels were measured to ensure equal protein loading. Relative quantification (RQ) analyses of the induction in the ratio of Bcl-2/Bax (F), and protein levels of cleaved caspase-9 (H) and cleaved caspase-3 (J) showed that 10 μM resveratrol increased the ratio of Bcl-2/Bax and decreased protein levels of cleaved caspase-9 and cleaved caspase-3 in a dose-dependent manner. Values obtained from three independent experiments are expressed as the mean ± SD. $^{*}P < 0.05$ vs. control; $^{**}P < 0.01$ vs. control; $^{\#}P < 0.05$ vs. OGD/R.

cleaved caspase-3 ($P < 0.01$ vs. control) (**Fig. 6I,J**). Conversely, 5 or 10 μM resveratrol in OGD/R-injured cells brought about an increased Bcl-2/Bax ratio and decreased protein levels of cleaved caspase-9 and cleaved caspase-3 in a dose-dependent manner. Cells treated with 5 or 10 μM resveratrol alone did not show any significant difference compared with the control ($P > 0.05$ vs. control).

Discussion

Previous studies have demonstrated the neuroprotective properties of resveratrol [6]. For instance, administration of resveratrol to culture medium protects a wide variety of neuronal cell types from oxidative stress-induced injury [7–9]; dietary supplementation of resveratrol can ameliorate neuronal damage and death resulted from oxidative stress in rodents [10]. However, these studies have not fully explored the specific molecular mechanisms by which resveratrol acts at the cellular level. Our study demonstrated that resveratrol exerted neuroprotective potential in OGD/R-induced PC12 cell apoptosis through mitochondrial-mediated signaling pathway.

There is compelling evidence that neuronal cells in the region of ischemic penumbra suffer transiently reversible damage and then eventually undergo delayed neuronal death by apoptosis [2]. Consequently, the salvageable neuronal damage offers a possibility for therapeutic intervention. To develop potential protective agents for stroke therapy and understand the mechanisms of neuronal apoptosis after ischemic insult, *in vitro* cell culture model of ischemia using PC12 cells has been established [11]. These cells are sensitive to OGD/R injury [20]; therefore, they are suitable for the investigation of the effects of resveratrol on OGD/R-induced cytotoxicity. The experimental procedure includes an initial short phase (6 h) of oxygen and glucose deprivation (OGD), followed by a prolonged phase (24 h) of restoration (R). Our results showed that apoptosis was the major pattern of cell death induced by OGD/R. Resveratrol significantly improved cell viability and protected PC12 cells against apoptosis induced by OGD/R at the optimal protective concentration of 10 μM.

Previous observations have demonstrated that the rate of ROS formation is equal to that of their elimination in neuronal cells under normal condition [21]. Mitochondria play a pivotal role in maintaining the redox balance. Superoxide generated from mitochondrial respiratory chain Complex I and Complex III is the major component of intracellular ROS [22], and excessive mitochondrial superoxide can be converted into hydrogen peroxide, which is subsequently broken down to oxygen and water [23]. However, during ischemia and reperfusion, the redox balance is perturbed by excessive intracellular ROS generated following mitochondrial superoxide accumulation due to mitochondrial dysfunction [24], which is a well-known etiological factor involved in oxidative stress-induced neuronal apoptosis [25]. Thus, it is of interest to identify the contribution of mitochondria to OGD/R-induced ROS production. Consequently, the present study showed that OGD/R caused a marked rise in oxidative stress as characterized by excessive intracellular ROS and mitochondrial superoxide accumulation, which were attenuated by resveratrol. In addition, the capability of resveratrol in decreasing membrane lipid peroxidation and restoring enzymatic antioxidant defense further suggested its antioxidant property in neuroprotection.

Excessive intracellular ROS triggers a significant activation of signal transduction cascades to cause a disturbance of $[Ca^{2+}]i$ homeostasis [3], leading to alteration of energy metabolism, and the subsequent initiation of apoptosis [26]. $[Ca^{2+}]i$ and intracellular ROS signaling systems are intimately integrated; components of intracellular ROS homeostasis that depend on $[Ca^{2+}]i$ regulation may influence intracellular redox balance, and vice versa [27]. This study demonstrated that resveratrol inhibited the overload of $[Ca^{2+}]i$ and the generation of intracellular ROS, which were pivotal steps in combating OGD/R-induced apoptosis.

Mitochondrion, as a very efficient $[Ca^{2+}]i$ buffer, takes up substantial amounts of $[Ca^{2+}]i$ at the expense of MMP [28], causing an obvious decrease in MMP. In addition, the extensive production of intracellular ROS can also damage the mitochondrial membrane lipids, which might be one of the inducers of MMP reduction. Consequently, disruption of MMP triggers the pathological opening of MPTP and excessive MPTP opening leads to the further collapse of the MMP. This vicious circle may result in mitochondrial swelling, rupture of the outer mitochondrial membrane, and the consequent release of cytochrome c from mitochondria into cytosol, which ultimately activates caspase cascade and induces apoptosis [8]. In accordance with the previous experimental results [29], we also found that OGD/R caused the disruption of MMP, the pathological opening of MPTP, and the release of cytochrome c from mitochondria, suggesting that mitochondrial-mediated signaling pathway may have a determinant role in OGD/R-induced neurotoxicity. Importantly, resveratrol efficiently maintained the MMP, reversed the uncontrolled opening of MPTP, and prevented the cytochrome c release in the presence of OGD/R, which strengthened the notion that resveratrol restored OGD/R-induced dysfunction of mitochondria by attenuating the impairment of mitochondrial membrane.

As a mitochondrial membrane-associated protein, the Bcl-2 exerts regulating effects on cellular activity after a variety of physiological and pathological insults, and is suggested to be directly dependent on the elevation of Bax and its translocation to the mitochondrial membrane [30]. When being translocated to the mitochondrial membrane, Bax homodimerizes and drives the activation of terminal caspases such as caspase-9 and caspase-3 by exacerbating mitochondrial membrane damage [8]. Conversely, the formation of the Bcl-2/Bax heterodimer can prevent or reduce some of these downstream events by a series of reactions. In this regard, the ratio of Bcl-2/Bax may predict the anti-apoptotic fate of the cell better than the absolute concentrations of either molecule alone [31]. Our results indicated that OGD/R-induced PC12 cell apoptosis was characterized by the decreased ratio of Bcl-2/Bax and subsequently increased protein levels of cleaved caspase-9 and cleaved caspase-3. Reversal of these trends by resveratrol suggested that the anti-apoptosis activity of resveratrol was intervened through the mitochondria-mediated signaling pathway in PC12 cells.

In should be noted that there are some limitations in this study. First, we do not compare the antioxidative effects of resveratrol with the other potent antioxidants that have been used clinically. Second, although well-differentiated PC12 cells are widely applied to study cellular hypoxia toxicity and are more sensitive to OGD/R injury, the cell model cannot totally represent the characters of primary cultured neurons. Therefore, further studies focusing directly on primary neurons *in vivo* models are encouraged.

In summary, we have demonstrated that resveratrol could protect PC12 cells against OGD/R-induced injury through its anti-apoptotic effect, which is partially attributed to the mitochondrial-mediated signaling pathway including attenuating intracellular ROS and mitochondrial superoxide accumulation, preserving $[Ca^{2+}]i$ homeostasis, ameliorating MMP dissipation, blocking MPTP opening, inhibiting the mitochondrial cytochrome c release, and modulating the protein levels of Bcl-2 family and terminal caspases. These mechanisms may act individually or in a concerted fashion. Our study provides new hopes in the development of a promising therapeutic approach for preventing acute brain damage associated with cerebral ischemia and warrants further investigations in both pre- and post-ischemic treatment *in vivo*.

Funding

This work was supported by the grants from the 2013-2014 National Clinical Key Specialty Construction Project, the Health

Bureau Scientific Research Foundation of Shanghai (No. GWDTR201219), and the Shanghai Committee of Science and Technology (No. 13DZ1941003).

References

1. Flynn RW, MacWalter RS, Doney AS. The cost of cerebral ischaemia. *Neuropharmacology* 2008, 55: 250–256.
2. Rosso C, Samson Y. The ischemic penumbra: the location rather than the volume of recovery determines outcome. *Curr Opin Neurol* 2014, 27: 35–41.
3. Hou T, Zhang X, Xu J, Jian C, Huang Z, Ye T, Hu K, *et al*. Synergistic triggering of superoxide flashes by mitochondrial Ca2+ uniport and basal reactive oxygen species elevation. *J Biol Chem* 2013, 288: 4602–4612.
4. Fong MY, Jin S, Rane M, Singh RK, Gupta R, Kakar SS. Withaferin A synergizes the therapeutic effect of doxorubicin through ROS-mediated autophagy in ovarian cancer. *PLoS One* 2012, 7: e42265.
5. Okamura K, Tsubokawa T, Johshita H, Miyazaki H, Shiokawa Y. Edaravone, a free radical scavenger, attenuates cerebral infarction and hemorrhagic infarction in rats with hyperglycemia. *Neurol Res* 2014, 36: 65–69.
6. Liu Y, He XQ, Huang X, Ding L, Xu L, Shen YT, Zhang F, *et al*. Resveratrol protects mouse oocytes from methylglyoxal-induced oxidative damage. *PLoS One* 2013, 8: e77960.
7. Fukui M, Choi HJ, Zhu BT. Mechanism for the protective effect of resveratrol against oxidative stress-induced neuronal death. *Free Radic Biol Med* 2010, 49: 800–813.
8. Agrawal M, Kumar V, Singh AK, Kashyap MP, Khanna VK, Siddiqui MA, Pant AB. trans-Resveratrol protects ischemic PC12 Cells by inhibiting the hypoxia associated transcription factors and increasing the levels of antioxidant defense enzymes. *ACS Chem Neurosci* 2013, 4: 285–294.
9. Zhang H, Schools GP, Lei T, Wang W, Kimelberg HK, Zhou M. Resveratrol attenuates early pyramidal neuron excitability impairment and death in acute rat hippocampal slices caused by oxygen-glucose deprivation. *Exp Neurol* 2008, 212: 44–52.
10. Wang LM, Wang YJ, Cui M, Luo WJ, Wang XJ, Barber PA, Chen ZY. A dietary polyphenol resveratrol acts to provide neuroprotection in recurrent stroke models by regulating AMPK and SIRT1 signaling, thereby reducing energy requirements during ischemia. *Eur J Neurosci* 2013, 37: 1669–1681.
11. Wu Y, Shang Y, Sun SG, Liu RG, Yang WQ. Protective effect of erythropoietin against 1-methyl-4-phenylpyridinium-induced neurodegenaration in PC12 cells. *Neurosci Bull* 2007, 23: 156–164.
12. Hu W, Wang G, Li P, Wang Y, Si CL, He J, Long W, *et al*. Neuroprotective effects of macranthoin G from Eucommia ulmoides against hydrogen peroxide-induced apoptosis in PC12 cells via inhibiting NF-κB activation. *Chem Biol Interact* 2014, 224C: 108–116.
13. Shen X, Tang Y, Yang R, Yu L, Fang T, Duan JA. The protective effect of Zizyphus jujube fruit on carbon tetrachloride-induced hepatic injury in mice by antioxidative activities. *J Ethnopharmacol* 2009, 122: 555–560.
14. Ungvari Z, Labinskyy N, Mukhopadhyay P, Pinto JT, Bagi Z, Ballabh P, Zhang C, *et al*. Resveratrol attenuates mitochondrial oxidative stress in coronary arterial endothelial cells. *Am J Physiol Heart Circ Physiol* 2009, 297: H1876–H1881.
15. Qu M, Nan X, Gao Z, Guo B, Liu B, Chen Z. Protective effects of lycopene against methylmercury-induced neurotoxicity in cultured rat cerebellar granule neurons. *Brain Res* 2013, 1540: 92–102.
16. Xiao X, Liu J, Hu J, Zhu X, Yang H, Wang C, Zhang Y. Protective effects of protopine on hydrogen peroxide-induced oxidative injury of PC12 cells via Ca2+ antagonism and antioxidant mechanisms. *Eur J Pharmacol* 2008, 591: 21–27.
17. Brugè F, Tiano L, Astolfi P, Emanuelli M, Damiani E. Prevention of UVA-induced oxidative damage in human dermal fibroblasts by new UV filters, assessed using a novel *in vitro* experimental system. *PLoS One* 2014, 9: e83401.
18. Sun Q, Jia N, Wang W, Jin H, Xu J, Hu H. Protective effects of astragaloside IV against amyloid beta1-42 neurotoxicity by inhibiting the mitochondrial permeability transition pore opening. *PLoS One* 2014, 9: e98866.
19. Gillies LA, Kuwana T. Apoptosis regulation at the mitochondrial outer membrane. *J Cell Biochem* 2014, 115: 632–640.
20. Negis Y, Unal AY, Korulu S, Karabay A. Cell cycle markers have different expression and localization patterns in neuron-like PC12 cells and primary hippocampal neurons. *Neurosci Lett* 2011, 496: 135–140.
21. Robert SM, Ogunrinu-Babarinde T, Holt KT, Sontheimer H. Role of glutamate transporters in redox homeostasis of the brain. *Neurochem Int* 2014, 73: 181–191.
22. Li J, Yu W, Li XT, Qi SH, Li B. The effects of propofol on mitochondrial dysfunction following focal cerebral ischemia-reperfusion in rats. *Neuropharmacology* 2014, 77: 358–368.
23. Sena LA, Chandel NS. Physiological roles of mitochondrial reactive oxygen species. *Mol Cell* 2012, 48: 158–167.
24. Sanderson TH, Reynolds CA, Kumar R, Przyklenk K, Hüttemann M. Molecular mechanisms of ischemia-reperfusion injury in brain: pivotal role of the mitochondrial membrane potential in reactive oxygen species generation. *Mol Neurobiol* 2013, 47: 9–23.
25. Tao L, Li X, Zhang L, Tian J, Li X, Sun X, Li X, *et al*. Protective effect of tetrahydroxystilbene glucoside on 6-OHDA-induced apoptosis in PC12 cells through the ROS-NO pathway. *PLoS One* 2011, 6: e26055.
26. Hsieh YF, Liu GY, Lee YJ, Yang JJ, Sándor K, Sarang Z, Bononi A, *et al*. Transglutaminase 2 contributes to apoptosis induction in jurkat T cells by modulating Ca2+ homeostasis via cross-linking RAP1GDS1. *PLoS One* 2013, 8: e81516.
27. Tang DW, Fang Y, Liu ZX, Wu Y, Wang XL, Zhao S, Han GC, *et al*. The disturbances of endoplasmic reticulum calcium homeostasis caused by increased intracellular reactive oxygen species contributes to fragmentation in aged porcine oocytes. *Biol Reprod* 2013, 89: 124.
28. Sun Z, Han J, Zhao W, Zhang Y, Wang S, Ye L, Liu T, *et al*. TRPV1 activation exacerbates hypoxia/reoxygenation-induced apoptosis in H9C2 cells via calcium overload and mitochondrial dysfunction. *Int J Mol Sci* 2014, 15: 18362–18380.
29. Ji HJ, Wang DM, Hu JF, Sun MN, Li G, Li ZP, Wu DH, *et al*. IMM-H004, a novel courmarin derivative, protects against oxygen-and glucose-deprivation/restoration-induced apoptosis in PC12 cells. *Eur J Pharmacol* 2014, 723: 259–266.
30. Edlich F, Banerjee S, Suzuki M, Cleland MM, Arnoult D, Wang C, Neutzner A, *et al*. Bcl-x(L) retrotranslocates Bax from the mitochondria into the cytosol. *Cell* 2011, 145: 104–116.
31. Cory S, Adams JM. The Bcl2 family: regulators of the cellular life-or-death switch. *Nat Rev Cancer* 2002, 2: 647–656.